Coexistence of Two Granular Temperatures in Binary Vibrofluidized Beds

R. D. Wildman[1] and D. J. Parker[2]

[1]*School of Mechanical and Manufacturing Engineering, Loughborough University, Loughborough, Leicestershire, LE11 3TU, United Kingdom*

[2]*School of Physics and Astronomy, University of Birmingham, Edgbaston, Birmingham, B15 2TT, United Kingdom*

(Received 24 May 2001; revised manuscript received 28 November 2001; published 25 January 2002)

An investigation into the granular temperature distributions of a binary vibrofluidized granular bed has been conducted using positron emission particle tracking. By repeating each experiment with the tracer selected in turn from the two size components, the granular temperature and packing fraction distributions for each phase were determined. It was found that, for a range of size fractions, the granular temperature of the larger particles was higher than that of the smaller diameter grains, a result which was supported by a simple theoretical analysis based on the steady state energy equation.

DOI: 10.1103/PhysRevLett.88.064301 PACS numbers: 45.70.Mg, 47.20.Bp, 51.10.+y

Vibrofluidized beds are often employed as idealized systems for observing the fundamental mechanics of granular flows [1]. In two dimensions, the use of high speed digital photography has enabled fluidized granular beds to be studied at the single particle level and allowed the concept of the kinetic theory approach to be investigated and validated [2–4]. Recently, a number of techniques have been applied to study three-dimensional fluidized granular systems [5–8]. In particular, positron emission particle tracking (PEPT) has provided researchers with an insight into the internal dynamics of vibrofluidized beds at unprecedented spatial and temporal resolution [9]. This has led to the first measurements of granular temperature profiles, combined with whole field determination of packing fraction distributions [5,10]. In three dimensions it is possible to observe the behavior of more than one species, and in this Letter we show that two granular temperatures can coexist in binary systems; the dissipative and thus nonequilibrium nature of granular flows does not allow the interdispersed granular gases to relax towards a single temperature. These results are supported by theoretical analysis of the steady state energy balance equation.

Fluidized granular systems are often characterized in terms similar to those used for study of thermal fluids, e.g., density and granular temperature. Here granular temperature is defined in terms of the mean square velocity of the grains, in direct analogy with thermodynamic systems, though one must note that in a granular system only momentum is conserved; kinetic energy is lost through dissipation of energy into heat and deformation during collisions [11]. This dissipation allows a wide range of unexpected phenomena to become apparent, such as convection [9,12], departures from Fourier's law for the heat flux [13], and segregation [14,15]. Although this last effect has typically been studied in the context of low-amplitude vibrations, in the following text we demonstrate, for the first time in highly fluidized binary granular beds, that granular temperatures can be species dependent, with the differences being independent of material properties such as the restitution coefficient.

Experimentally, a three-dimensional vibrofluidized granular bed is generated by applying a vibration to a cylindrical cell, containing granular particles, using an electrodynamic shaker system [5]. This cell is 145 mm in diameter and 300 mm in height and shaken with a frequency of 50 Hz and an amplitude of 1.74 mm. The granular media consist of two sizes of ballotini glass spheres, 5.0 ± 0.2 mm and 4.0 ± 0.2 mm in diameter, d, restitution coefficients of $\varepsilon_1 = 0.91$ and $\varepsilon_2 = 0.91$, respectively. The quantity of grains is varied in the following proportions: $N_1/N_2 = 525/270$, $350/540$, and $175/810$, where N_1 is the number of 5 mm grains and N_2 is the number of 4 mm grains. The number of grains in a single layer is $N_1 \sim 700$ or $N_2 \sim 1080$. PEPT is used to follow the position of a single tracer particle for a period of $\sim$30 min. For each ratio N_1/N_2 two sets of data are recorded, first tracking a 5 mm grain and second a 4 mm grain. In each case the selected grain is labeled with $\sim$8 MBq of the positron emitting radionuclide ^{18}F [generated in the reaction ^{16}O(^{3}He, p)^{18}F when the glass bead is irradiated by a 33 MeV ^{3}He cyclotron beam] and is returned to the bed. A positron camera consisting of a pair of digital NaI(Tl) gamma cameras operating in coincidence [16] is used to detect the pairs of back-to-back gamma rays emitted from electron-positron annihilation (Fig. 1). Coincidence data are recorded in list mode at a rate of up to 100k events per second. From a sample of $\sim$100 events (i.e., at 1 kHz), the tracer location can be determined to an accuracy of around 1 mm using an iterative algorithm that discards the background of scattered data [17].

The packing fraction is determined from the time-residence distribution of the tracer particle, through an assumption that the system is ergodic; i.e., an ensemble average is proportional to a temporal average [5]. Figure 2 shows the packing fraction distribution for $N_1/N_2 = 525/270$, where Fig. 2a shows the distribution of 5 mm

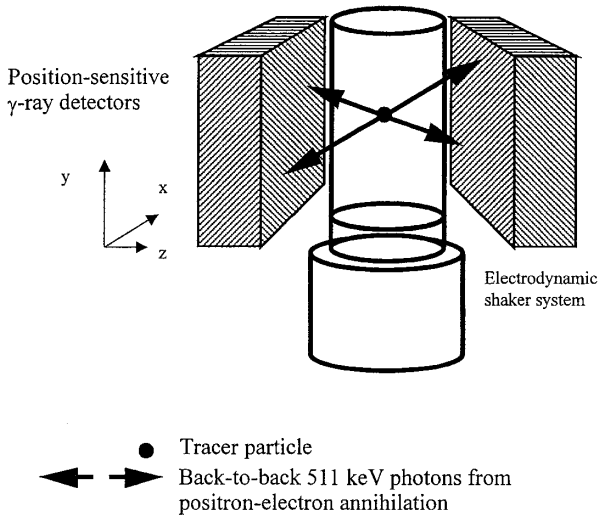

FIG. 1. Schematic of the positron emission particle tracking facility. A positron-emitting radioactive particle is used as the tracer bead. Back-to-back gamma rays, resulting from electron-positron annihilation events, are detected by the gamma cameras. The coordinates of the tracer particle can then be determined via triangulation of successive location events.

grains ($N_1 = 525$) and Fig. 2b shows the distribution of 4 mm particles ($N_2 = 270$). Also shown are the mean velocity fields for each species. These figures show clearly the variations in the radial density distribution near the wall and the existence of the convection rolls noted previously [9]. The granular temperature is typically calculated by direct determination of the mean square velocity about the mean [18]. However, in this case, we employ the more robust technique of extracting the mean square velocity from the ballistic portion (short time) of the mean squared displacement of the grain [2,5,9,10,19]. This has the advantage that one does not need to detect grain collisions, nor is it necessary to numerically differentiate the coordinate traces. Figure 3 shows the granular temperature measurements performed for each ratio of N_1 to N_2. The granular temperature profiles are characteristic of those observed in vibrated granular beds: dissipation results in a declining profile that converges towards an asymptotic temperature [2,5,9,10,18–23]. However, one can clearly see from Fig. 3 that in general $T_1 > T_2$. In a thermal system, the zeroth law of thermodynamics means that the temperatures must equilibrate. However, in a nonequilibrium steady state, such as in a vibrofluidized bed, the granular temperature is determined by the balance of kinetic energy entering into the system through grain-base collisions and kinetic energy being dissipated in the bulk and at the walls. In a binary system one also has to make the distinction between collisions between like and unlike grains: differences in packing fraction distributions (shown in Fig. 2) and thus also collision and dissipation rates will lead to differences in the granular temperatures of the two species. Estimates of the ratio of the granular temperatures for each species can be estimated from the energy input-dissipation

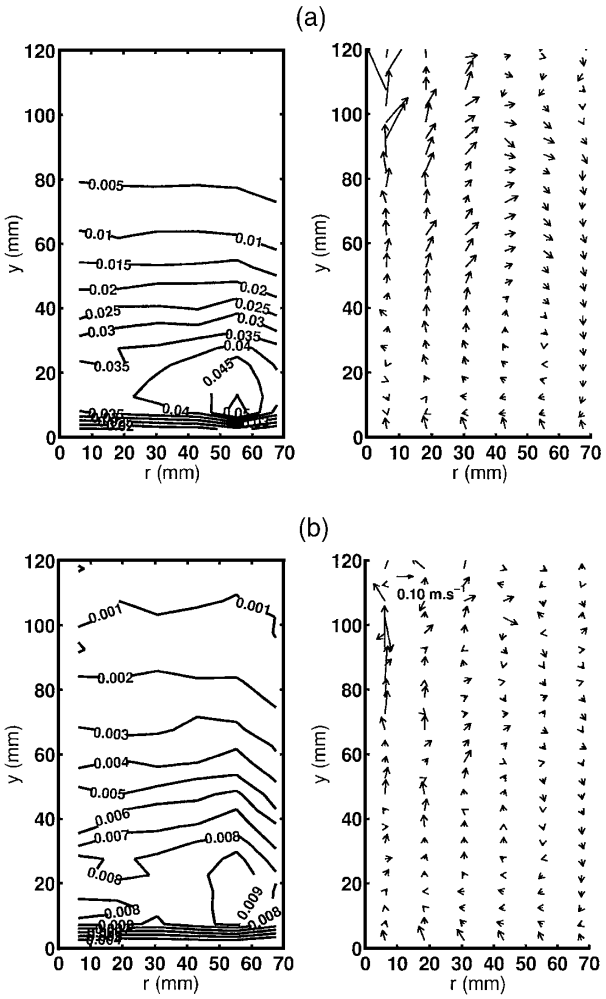

FIG. 2. Packing fraction contour maps (left) with the mean velocity field (right) for (a) $N_1 = 525$ and (b) $N_2 = 270$ for the combination 525/270 (5 mm/4 mm). The data have been averaged about the azimuthal angle resulting in a distribution being projected onto the r-y plane. The figures clearly show the variation in packing fraction both as a function of altitude and radial distance from the axis ($r = 0$). Convection rolls exist for both species, with the focus a few particle diameters from the wall.

relationship:

$$\dot{E}_{\mathrm{I}}^{i} = D_{\mathrm{gg}}^{ii} + D_{\mathrm{gg}}^{ij} + D_{\mathrm{gw}}^{i}, \tag{1}$$

where $\dot{E}_{\mathrm{I}}^{i}$ is the energy input rate, D_{gg}^{ii} and D_{gg}^{ij} are the dissipation rates due to grain-grain collisions, and D_{gw}^{i} is the dissipation rate due to grain-wall collisions. The i and j superscripts refer to the granular species where $i \neq j$. The analysis is simplified by assuming an isothermal temperature distribution and by ignoring the grain-wall dissipation. The D_{gg}^{ii} terms are calculated by determining the grain-grain collision rates and integrating over the packing fraction distribution to estimate the total dissipation rate [20–22], and the energy input rate is determined from analysis of single particle dynamics at the base [22,23]. In

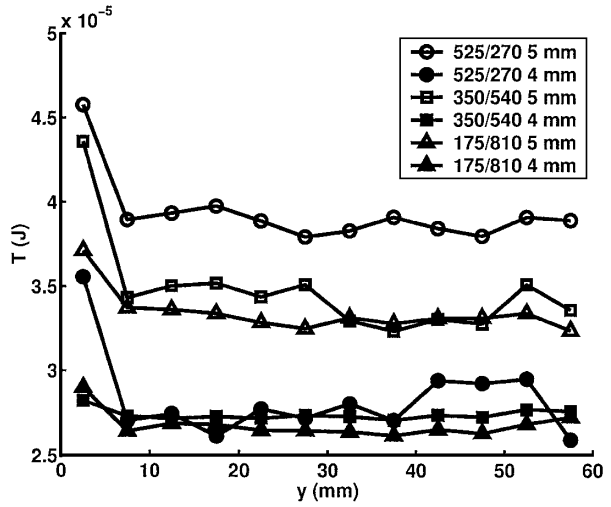

FIG. 3. Granular temperature profiles for $N_1/N_2 = 525/270$, 350/540, and 175/810 (5 mm/4 mm), for grains within a central core, $r < 30$ mm.

order to ease the analysis of the dissipation due to the D_{gg}^{ij} terms, we make the assumption that an effective temperature, T^*, may be used to predict the collision rate of unlike grains. Jenkins and Mancini have similarly employed an effective temperature, using a weighted mean dependent on the number fraction of each species [24] and Lu *et al.* have also shown that one may predict the collision rate of two species at different temperatures using the Chapman-Enskog method [25]. These approaches, however, quickly lead to complexities that increase the difficulties in solving Eq. (1) for the temperature of each species, and we have employed a coarser method, where $T^* = (T_1 + T_2)/2$ to elucidate general trends in the granular gas behavior. This qualitative approach results in two coupled equations for T_1 and T_2. In this case, the interspecies dissipation, D_{gg}^{ij}, is proportional to $(1 + T_1/T_2)^{3/2}$, which using a Taylor expansion about $T_1/T_2 = 1$ can be approximated as $\sim(1/\sqrt{2})(1 + 3T_1/T_2)$, enabling the coupled equations to be expressed in the form

$$T_i^2 + T_i(\alpha T_j + \beta) + \gamma T_j = 0, \tag{2}$$

where α, β, and γ are species dependent functions of grain mass, number, diameter, restitution coefficient, and cross-sectional area of the cell. Equation (2) can be solved, via substitution and implementation of a Newton-Raphson root locating procedure, for the temperature of each species. A similar procedure was undertaken to include the wall dissipation. However, for grain-wall restitution coefficients of $\varepsilon_W < 0.999$, a physically realistic solution was not possible using this simplified approach. These analyses are compared to theory for which interspecies collisions are not accounted for [22]. Under these conditions the granular temperature ratio simplifies to

$$\frac{T_1}{T_2} \approx \frac{N_2(1 - \varepsilon_2)d_1}{N_1(1 - \varepsilon_1)d_2}, \tag{3}$$

the results of which for the given experimental parameters are shown in Table I.

The comparison of the experimental and theoretical results is shown in Table I. The theory is not expected to produce accurate predictions due to the simplifications employed; rather its use lies in elucidating the qualitative trends in the grain behavior. We see that despite the correspondence not being exact, which one might expect due to the assumption of an isothermal granular temperature and Boltzmann packing distribution, the inclusion of interspecies collisions in the theoretical analysis does surprisingly well at predicting the granular temperature ratio and is able to predict the correct trend. In contrast, however, neglecting the interspecies collisions means that the granular temperature scales as $(N_1/N_2)^{-1}$, predicting both a rising trend in the ratio of the granular temperatures with fraction of small grains and that the ratio may become <1. In both the experimental and theoretical cases the grain-grain restitution coefficients are similar (for theory $\varepsilon_1 = \varepsilon_2 = 0.91$), suggesting that the divergence of the granular temperature distributions is driven, in this case, not by differences in the restitution coefficients as might be expected, but as a result of the different packing fraction distributions and hence, collision and dissipation rates, for each species. This is in obvious contrast to thermal systems where the system would equilibrate to a single temperature. One also sees that the complex boundary conditions in granular systems play a role in determining the granular temperature. In a thermal system, the local temperature at the boundary must be identical for both species, but for a granular gas, the dissipation at the wall is dependent on the collision rate, which, in turn, depends on the local temperature and density of each species. Thus, the differences in the dissipation rates, at the wall and within the bulk of the granular gas, allow the system to relax towards separate

TABLE I. Comparison of the experimental results and theoretical predictions for the granular temperature ratio, T_1/T_2, in binary vibrofluidized granular beds.

N_1/N_2	T_1/T_2 experiment	T_1/T_2 theory without wall dissipation	T_1/T_2 theory with wall dissipation ($\varepsilon_W = 0.999$)	T_1/T_2 theory, no interspecies collisions
525/270	1.41	4.11	3.30	0.41
350/540	1.27	2.43	2.27	1.23
175/810	1.25	1.43	1.59	3.70

granular temperatures. These results have important ramifications for prediction of behavior in industrial systems where distributions of particle sizes are used and granular temperature would also be distributed among the grain sizes.

The work was funded by the Engineering and Physical Sciences Research Council under Contract No. GR/L61781 and by Shell International Oil Products B.V. The authors thank Professor Jean-Pierre Hansen and Professor Jonathan Huntley for useful discussions.

[1] C. S. Campbell, Annu. Rev. Fluid Mech. **22**, 57 (1990).
[2] R. D. Wildman, J. M. Huntley, and J.-P. Hansen, Phys. Rev. E **60**, 7066 (1999).
[3] L. Oger, C. Annic, D. Bideau, R. Dai, and S. B. Savage, J. Stat. Phys. **82**, 1047 (1996).
[4] E. Azanza, F. Chevoir, and P. Moucheront, J. Fluid Mech. **400**, 199 (1999).
[5] R. D. Wildman, J. M. Huntley, J.-P. Hansen, D. J. Parker, and D. A. Allen, Phys. Rev. E **62**, 3826 (2000).
[6] N. Menon and D. J. Durian, Science **275**, 1920 (1997).
[7] E. E. Ehrichs, H. M. Jaeger, G. S. Karczmar, J. B. Knight, V. Y. Kuperman, and S. R. Nagel, Science **267**, 1632 (1995).
[8] J. D. Seymour, A. Caprihan, S. A. Altobelli, and E. Fukushima, Phys. Rev. Lett. **84**, 266 (2000).
[9] R. D. Wildman, J. M. Huntley, and D. J. Parker, Phys. Rev. Lett. **86**, 3304 (2001).
[10] R. D. Wildman, J. M. Huntley, and D. J. Parker, Phys. Rev. E **63**, 061311 (2001).
[11] C. S. Campbell, J. Fluid Mech. **348**, 85 (1997).
[12] R. Ramirez, D. Risso, and P. Cordero, Phys. Rev. Lett. **85**, 1230 (2000).
[13] R. Soto, M. Mareschal, and D. Risso, Phys. Rev. Lett. **83**, 5003 (1999).
[14] N. Shishodia and C. R. Wassgren, Phys. Rev. Lett. **87**, 084302 (2001).
[15] J. B. Knight, H. M. Jaeger, and S. R. Nagel, Phys. Rev. Lett. **70**, 3728 (1993).
[16] D. J. Parker, R. N. Forster, P. Fowles, and P. S. Takhar, Nucl. Instrum. Methods Phys. Res., Sect. A **477**, 540 (2002).
[17] D. J. Parker, C. J. Broadbent, P. Fowles, M. R. Hawkesworth, and P. A. McNeil, Nucl. Instrum. Methods Phys. Res., Sect. A **236**, 592 (1993).
[18] S. Warr, G. T. H. Jacques, and J. M. Huntley, Powder Technol. **81**, 41 (1994).
[19] R. D. Wildman and J. M. Huntley, Powder Technol. **113**, 14 (2000).
[20] P. Sunthar and V. Kumaran, Phys. Rev. E **60**, 1951 (1999).
[21] V. Kumaran, Phys. Rev. E **57**, 5660 (1998).
[22] S. Warr, J. M. Huntley, and G. T. H. Jacques, Phys. Rev. E **52**, 5583 (1995).
[23] V. Kumaran, J. Fluid Mech. **364**, 163 (1998).
[24] J. T. Jenkins and F. Mancini, Phys. Fluids A **1**, 2050 (1989).
[25] H. L. Lu, W. T. Liu, R. S. Bie, L. D. Yang, and D. Gidaspow, Physica (Amsterdam) **284A**, 265 (2000).